Published in final edited form as:
Mol Ther. 2008 September ; 16(9): 1580–1586. doi:10.1038/mt.2008.148.

Adeno-Associated Viral Vector Mediated Gene Delivery of Endothelin Converting Enzyme Reduces Aβ Deposits in APP +PS-1 Transgenic Mice

Carty N.[1], **Nash K.**[2], **Lee D.**[1], **Mercer M.**[1], **Gottschall P.E.**[3], **Meyers C.**[2], **Muzyczka N.**[2], **Gordon M.N.**[1], and **Morgan D.**[1]

[1]Alzheimer's Research Laboratory, Department of Molecular Pharmacology and Physiology, School of Biomedical Sciences, University of South Florida College of Medicine, 12901 Bruce B Downs Blvd, Tampa, FL 33612, USA.

[2] Department of Molecular Genetics and Microbiology, University of Florida College of Medicine, Box 100266, Gainesville FL 32610

[3] University of Arkansas for Medical Sciences Department of Pharmacology and Toxicology, Slot #611, 4301 West Markham Street Little Rock, Arkansas 72205−7199

Abstract

Reduction of Aβ deposition is a major therapeutic strategy in Alzheimer's disease (AD). The concentration of Aβ in the brain is modulated, not only by Aβ production, but also by its degradation. One protease involved in the degradation of Aβ peptides is endothelin converting enzyme (ECE). In the current study, we investigated the effects of an intracranial administration of a recombinant adeno-associated viral vector (rAAV) containing the ECE-1 gene on amyloid deposition in amyloid precursor protein (APP) plus presenilin-1 (PS1) transgenic mice. The recombinant AAV vector was injected unilaterally into the right anterior cortex and hippocampus of six-month-old mice while control mice received an AAV vector expressing GFP. Immunohistochemistry for the haemagglutinin tag appended to ECE revealed strong expression in areas surrounding the injection sites but minimal expression in the contralateralregions. Immunohistochemistry for Aß decreased in the anterior cortex and hippocampus of mice receiving ECE cDNA. Further, decreases in Congo red positive deposits were also observed in both regions. These results indicate that increasing the expression of β-amyloid degrading enzymes through gene therapy is a promising therapeutic avenue through which to treat AD.

Keywords

Alzheimer's disease; Beta Amyloid; Gene Therapy; Viral Vector; Amyloid Degrading Enzyme; Zinc Metalloprotease

Introduction

AD is the most common form of senile dementia (a group of conditions that gradually destroy brain cells leading to progressive decline in mental capacity) affecting approximately 4.5 million individuals in the United States. The molecular mechanisms underlying AD have been

Corresponding Author: Dave Morgan, Alzheimer's Research Laboratory, University of South Florida College of Medicine, 12901 Bruce B Downs Blvd MDC Box 9, Tampa, FL 33612, USA Phone: +1 (813) 974−3949; Fax: +1 (813) 974−3079. Email: E-mail: scientist.dave@gmail.com.

extensively investigated [1]. Although the mechanism by which neuritic plaques and neurofibrillary tangles can eventually lead to neuron loss is debated, it has been repeatedly demonstrated that reducing amyloid deposits in the brain can significantly improve cognitive deficits in amyloid depositing transgenic mice [2,3,4,5]. Consequently, elucidating novel methods of decreasing or preventing amyloid accumulation has been a primary focus in the treatment of AD.

In recent years several endogenous proteases have been found which degrade Aβ in the brain and other tissues both *in vivo* and *in vitro*. These zinc metalloproteases, include neprilysin (NEP), insulin degrading enzyme (IDE; insulysin), and endothelin converting enzymes (ECE-1 and ECE-2). Other proteases that appear to play a role in Aß metabolism include matrix metalloproteinase-9 [6], cathepsin B [7] and plasmin [8]. The overall accumulation of Aβ in the brain is attributed to an imbalance between its production and degradation/clearance. Down-regulation of these degrading enzymes within the brain during aging could potentially contribute to Aβ accumulation eventually leading to development of AD [9,10].

Several current studies have implicated ECE as an important enzyme in the degradation of Aβ and preventing its accumulation [11]. ECE is a membrane-bound metalloprotease with an N-terminal cytosolic domain and an extracellular catalytic domain. ECE-1 is expressed in endothelial cells in all organs as well as other cell types including neurons, glia and neuroendocrine cells. Two different genes encoding for ECE-1 and ECE-2 have been identified, however ECE-1 is predominately expressed. ECE was discovered for its ability to catalyze the conversion of big endothelin into vasoactive endothelins [12, 13, 14, 15,16]. ECE-1 has now been reported to hydrolyse other biologically active peptides including bradykinin, neurotensin and substance P. In humans, ECE-1 exists as four different isoforms including ECE-1a, ECE-1b, ECE-1c,and ECE-1d [15,168,17]. Expression patterns have shown that these isoforms have distinct subcellular localizations with slight variations depending on the species and cell type[15,16]. To date, there are no significant differences reported in the catalytic properties of the different isoforms [8]. The Aβ degrading capability of ECE was discovered when Eckman [11] observed that the ECE inhibitor, phosphoramidon, caused a rapid accumulation of Aβ in a cell line expressing ECE but not in cells lacking ECE expression. Subsequent studies revealed that overexpression of ECE in cell lines reduced Aβ accumulation by approximately 90%. *In vivo* data from ECE (+/−) transgenic mice, which show 25% reductions in ECE-1 activity, also show significant increases in both Aβ40 and Aβ42 levels in the brain [11]. Moreover, intraventricular injections of phosphoramidon, increase Aß in wild type and APP transgenic mice [18]. These studies indicate a clear correlation between ECE-1 activity and Aβ load in the brain.

In the present study we investigated the effects of upregulating the ECE-1 enzyme by using a rAAV vector, serotype 5, on Aβ load in the brain. rAAV vectors are desirable candidates for gene therapy in the central nervous system because AAV is a nonpathogenic virus; it has low immunogenicity and it is deficient for replication due to the removal of all the viral encoded genes. Further, rAAV vectors have been shown to be very efficient in infecting neuronal cells and maintaining long term expression [19, 20]. We observed a significant reduction in the levels of Aα in the mice injected with the ECE virus which shows that this method may offer a promising therapeutic avenue through which to treat AD.

Results

The ECE-1 cDNA within the rAAV was under the control of the hybrid chicken β-actin cytomegalovirus (CBA) promoter and was tagged with haemagglutinin (HA) peptide sequence for detection within the brain and discrimination from endogenous ECE. Prior to virus production the rAAV vector was tested in HEK 293 cells to evaluate the expression cassette.

Cell lysate and conditioned media from transfected and untransfected cells were examined by Western blot analysis to determine ECE expression. Untransfected cell lysate and media were negative for ECE-HA protein expression. ECE-HA protein expression was only detected in the cell lyate fraction and not the media (Fig 1b).

The rAAV ECE vector was tested for enzyme activity in vivo. Nontransgenic mice (n=12) aged 9 months were injected bilaterally into the right and left hippocampus. Group one received the rAAV-ECE treatment and the second group served as the control group and received no treatment (n=6 per group). All injections were performed as described in Methods with each site of injection receiving a total volume of 2 μl of the vector at a concentration of 1×10^{12} vg/ml. Six weeks post injection the animals were sacrificed and frozen hippocampal tissue from the animals was homogenized and separated into membrane and soluble fractions by centrifugation. The ECE specific activity was determined as the nmole of MOCA/ min/μg protein. Within the homogenate and in the membrane fractions of the homogenized tissue, animals receiving the ECE treatment had significantly higher ECE-like specific activity than the control animals (Fig 2).

rAAV was initially injected unilaterally into the right hippocampus and right anterior cortical regions of six month old APP + PS1 mice. Each injection site received 2μl volume and a concentration of 1×10^{12} vg/ml of material at a flow rate of 0.5 μl/min. The expression of ECE was evaluated six weeks following treatment. Immunostaining of the tissue with an anti-HA antibody revealed ECE-HA expression in most animals. The gene expression patterns were confined to the areas surrounding the injection site. ECE-HA was detected in CA4 neurons in the hilus and CA3 neurons of the hippocampus pyramidal cell layer. In the dentate molecular layer, a number of round cells, possibly, oligodendrocytes or astrocytes also expressed the label (Fig. 3b). In animals receiving the rAAV-GFP control vector there was no positive HA staining in the hippocampus, but the GFP expression pattern was comparable to that of the ECE vector (Fig 4). In animals receiving the rAAV expressing ECE-HA there were low levels of positive staining in the contra-lateral dentate gyrus (Fig. 3a).

When the cortical regions were analyzed for expression, there was a large amount of ECE-HA expression which was also detected over a larger area of the cortex. ECE positive expression was concentrated in the anterior cortex (Fig 3c), but was observed also in the striatum, corpus callosum and septum along the midline (Fig 3d) in the ipsilateral and contralateral hemispheres. In animals receiving rAAV-GFP, GFP was detected in a similar expression patterns as ECE-HA. GFP positive cells were limited to the areas immediately surrounding the injection site in both the cortex and the hippocampus and no GFP positive cells were seen in the contralateral hemisphere (Fig. 4b, 4d and 4f respectively). This data suggests that the rAAV vector serotype 5 is effective at transducing neuronal cell types in vivo and expressing significant amounts of recombinant ECE-1.

Our next goal was to evaluate the effects of a single intracranial administration of the rAAV-ECE vector in APP + PS1 transgenic mice, to determine the effect of over expression of the transgene on amyloid deposition. rAAV was injected unilaterally into the right anterior cortex and hippocampus of six month old mice while the left untreated hemisphere. The control group was treated with rAAV containing GFP. Total Aβ load was ascertained six weeks after intracranial injections by immunohistochemical methods using a polyclonal anti-Aβ antiserum which primarily recognizes the N-terminal domain of Aß, and thus labels both $A\beta_{1-40}$ and $A\beta_{1-42}$ (gift of Gottschall, PE, Univ of Arkansas). The regional Aβ distribution and density in APP+PS1 transgenic mice were similar to those reported by Gordon et al. [21].

Immunohistochemistry revealed darkly stained compact plaques and more lightly stained diffuse plaque deposits in the APP+PS1 animal tissue. Plaque deposition was distributed

throughout the cortical regions as well as in the hippocampus (although most concentrated in the molecular layers of the dentate gyrus and the CA1 region, surrounding the hippocampal fissure). Animals injected with the control rAAV-GFP showed Aβ immunohistochemical staining patterns throughout the cortex and hippocampus comparable to those of untreated APP transgenic mice of the same age (Fig 5a and 5b). A notable decrease in the amount of hippocampal Aβ staining was observed in animals injected with the rAAV expressing ECE six weeks after the time of injection when compared to animals injected with the control rAAV-GFP vector (Fig. 5c, 5d). The reductions in Aβ deposition were limited to the areas surrounding the cortical and hippocampal injection sites. ANOVA analysis of total Aß was significantly decreased by 50% in mice receiving ECE in both the hippocampus and the anterior cortex (Fig. 5e).

Congophilic plaque load was also analyzed following intracranial injections of rAAV vectors. The area of congophilic labeling was substantially less than Aβ immunochemistry, staining only compacted fibrillar Aβ deposits, as expected [21]. Figures 6c and 6d indicate that the positive congophilic staining for the mice receiving the ECE vector was visibly less, especially in the hippocampus, compared to the control animals. Quantification of the Congo red staining by ANOVA analysis revealed that animals receiving the ECE transgene showed significant reductions in the hippocampal region (46%) as well as reductions, although not quite significant, in the anterior cortex (30%; Fig 6e).

Discussion

There have been several gene therapy approaches examined for the treatment of Alzheimer's disease. Initial experiments were based on the observation that application of neuronal growth factors mediated neuroprotection and reduced the loss of cholinergic neurons in experimental lesion models [22;23]. Therefore, NGF genes have been delivered to the brain using recombinant viral vectors, such as AAV and lentivirus, or delivered via an *ex vivo* approach, with transformed fibroblasts or neuronal stem cells [24,25]. These studies have shown rescue of cholinergic neurons and are being further examined as a potential therapy. However, it is unlikely that NGF would cure AD because the widespread neuronal loss that occurs in the later stages of the disease would not be compensated by the early rescue of cholinergic neurons. NGF rescue of neurons is currently being examined in clinical trials because it offers a substantial decline in the rate of neuronal loss and could slow the progression of symptoms of Alzheimer's. Other growth factors that are also of potential interest in AD include brain-derived neurotrophic factor and neurotrophin-4/5 to address the neuronal loss in the cortex and hippocampus.

A second approach to treat Alzheimer's pathology involves the reduction of Aβ through immunization. It was observed that immunization against Aβ would result in a significant reduction in Aβ deposits and improve learning and memory deficits [3,2]. Peripheral passive immunization against Aβ with antibody injections has been successful im mouse models and more recently viral vectors have been used as a gene therapy approach to deliver Aβ antibodies [26, 27]. This approach has demonstrated some promising reduction (25−50%) in the levels of Aβ deposition. AAVl vectors have also been used as an Aβ vaccine, with the over expression of Abeta42. This method has shown reduction in Aβ deposition and some reduction in cognitive impairment in Alzheimer Tg mice [28, 29, 30].

It has been demonstrated that the apolipoprotein E (apoE) gene is a major risk factor for late-onset AD with the ApoE2 allele decreasing and the ApoE4 allele increasing the morbid risk for developing AD. Therefore to develop a gene therapy approach to Alzheimer's, Dodart et al. (2005) over expressed ApoE2 using a lentiviral vector. The authors observed a dramatically

reduced hippocampal Aβ burden in Tg mice. It is as yet unclear how ApoE2 is reducing the Aβ but it may be increasing the Aβ clearance [31].

A final gene therapy approach for the treatment of Alzheimer's has been the over expression of Aβ degrading enzymes such as neprilysin. Either using a direct transduction of neurons using a viral vector or an ex vivo approach with transformed fibroblasts, the increase in NEP expression has been shown to significantly reduce the overall Aβ load on Alzheimer Tg mice [32, 33,34, 35]. In this report we are examining another Aβ degrading enzyme, ECE, for its ability to reduce the Aβ load on Alzheimer APP mice using rAAV for increased neuronal expression of ECE.

Recombinant AAV has become widely used for the transduction of neuronal cells. AAV is nonpathogenic, has low immunogenicity, lacks all viral genes and is capable of long term expression in neurons. This makes rAAV a good candidate for the use as a gene therapy vector for neurological disorders [20, 19]. Further, rAAV is currently being examined in a number of neurological clinical trials [36]. Here we are using rAAV for the expression of the ECE protease which had been previously shown to cleave Aβ peptide [11]. We believed that the over expression of ECE using rAAV would enable the clearance of Aβ deposition within the mouse brain and ameliorate the pathogenesis of Alzheimer's. rAAV serotype-5 ECE vector was injected unilaterally into the mouse hippocampus and anterior cortex. Examination of the expression profile of the expressed ECE has shown that the rAAV of ECE can transduce several different neuronal cell types within the mouse brain, and possible other cell types in the dentate molecular layer. This is consistent with the previously published serological specificity of this vector [37, 38,39]. The expression profile of ECE was similar to that observed with our rAAV5 vector expressing GFP.

Additionally, no noticeable toxic effects were seen in mice receiving the ECE vector compared to control animals. No neuron loss or gross morphometric changes were observed in fixed brain tissue. All animals were weighed before treatment and immediately before sacrifice and no significant changes in weight were noted indicating that up regulation of ECE does not appear to have adverse effects or cause general toxicity in the mouse model, yet further investigation must be done to confirm its safety profile. ECE has many endogenous peptides including opioid peptides, tachykinin, atrial naturetic peptides, and other small regulatory vasoactive peptides. It is uncertain whether interactions between other potential substrates in the brain may limit the ability of ECE to degrade Aβ or cause potential problems by reducing the levels of these other peptides. Previous studies have revealed that in the AD brain as well as in the animal model of AD, ECE (in addition to other Aβ degrading enzymes) are down regulated specifically in areas that are prone to plaque formation [40, 41]. Therefore, up-regulation of ECE to restore normal levels of this endogenous protease should have minimal adverse effects. In addition, ECE has been shown to have higher affinity for larger peptides such as bradykinin, substance P, and neurotensin, hydrolyzing them at amino acid hydrophobic residues [42, 43]. Monitoring changes in these peptides between control and treatment groups may help identify other potential toxic effects resulting from increases in ECE that could occur in this model.

Our results from the over expression of ECE suggest that the up-regulation of ECE through rAAV vectors can provide a viable method to decrease total amyloid deposition in the brain. The activity level determined using an ECE specific assay demonstrated that we achieved a several fold fold increase inECE activity in homogenates, most of which was membrane associated. This increase in ECE activity was able to significantly reduce total Aβ deposition in the anterior cortex and hippocampal sites of injection (Fig. 5). Similarly, when Congo red stained compacted deposits were measured; the ECE vector significantly reduced staining (Fig. 6). We were able to achieve a 50% reduction in the total Aβ present in the cortex and hippocampal regions. Similarly, we reduced the congophilic compact plaque load to ~50% of

that of the controls. We have yet to determine if this reduction in the Aβ levels in the mice with the ECE will lead to significant improvement in behavioral tests such as the Morris water maze. We are currently testing more injections of ECE to see if we can create a significant reduction of whole brain Aβ levels and ameliorate the memory deficits that are observed in the APP+PS1 mice. Our data are consistent with reports that ECE can degrade Aß in vitro, and that partial knockdown of the ECE gene leads to more rapid accumulation of Aß [44, 13]. The present work adds to the evidence that ECE plays an important role in Aß deposition by demonstrating that local over expression of the enzyme activity can dramatically reduce the deposition of amyloid in the brains of APP transgenic mice. Thus, regulation of ECE may be used as therapeutic target for the treatment of Alzheimer's disease.

Materials and Methods

Generation of ECE constructs and rAAV production

The ECE-1 gene (GI:4503442) was cloned using polymerase chain reaction (PCR) from a GenePool cDNA library obtained from Invitrogen. The primers used for the full length ECE were GAGGAATTCACCGGTCCACCATGCGGGGCGTGTGGCCGCCCCCGGTGTC and GAGATCGATTACCAGACTTCACACTTGTGAGGCGG. The PCR product was cloned into pBluescript and sequenced to confirm sequence identity. The ECE was then cloned into the vector called pTR5-MCS at the *Eco RI* and *Cla I* cloning sites. This vector contains the AAV terminal repeats for AAV virus production and the CBA promoter for ECE mRNA transcription. A Hemagglutinin (HA) tag was added to the C-terminus of ECE cDNA using the following oligonucleotide GTGTGAAGTCTGGATGGCTTCTAGCTATCTTATGACGTGCCTGACTATGCCATGT AA and its complement. The recombinant viruses were generated and purified using the method of Zolotukhin et al. (2002). Infectious rAAV particles are expressed as vector genomes (v/g)/ mL. Vector genomes were quantitated using the dot plot protocol, with a probe for the CBA promoter, as described by [47].

Western Blot analysis

Protein samples were boiled in Lamaelli sample buffer prior to loading on a 10% polyacrylamide gel. The proteins on the gel were transferred to Millipore Nitrocellulose membrane and probed with anti-HA antibody (Santa Cruz) and antimouse-HRP conjugate (Amersham). Millipore Immobilon detection reagent was used to visualize bands.

Transgenic mice

APP + PS1 mice [48] were acquired from the breeding colonies at the University of South Florida. Multiple mice were housed together whenever possible until the time of the experiment. Mice were then singly- housed 1 week before surgical procedures until the time of sacrifice. Study animals were given water and food *ad libitum* and maintained on a twelve hour light/dark cycle and standard vivarium conditions. Two cohorts of mice were used, the first cohort consisted of APP + PS1 mice aged 6 months (n =16) and the second cohort consisted of nontransgenic mice aged 9 months (n =12). Animals in each cohort were assigned to two groups. Group one received a control vector expressing GFP (first cohort n=8; second cohort n=6). Group two received AAV vector expressing native endothelin converting enzyme transgene (first cohort n =8; second cohort n=6). All groups were sacrificed after six weeks post intracranial injection.

Surgical procedure

Immediately before surgery mice were weighed then anesthetized using isoflurane. Surgery was performed using a stereotaxic apparatus. The cranium was exposed using an incision

through the skin along the median sagittal plane, and two holes were drilled through the cranium over the right cortex injection site and the right hippocampal injection site. Previously determined coordinates for burr holes, taken from bregma were as follows; frontal cortex, anteroposterior, −1.5 mm; lateral, −2.0 mm, vertical, 3.0 mm, hippocampus, anteroposterior, −2.7mm; lateral −2.5 mm, vertical, 3.0 mm. Burr holes were drilled using a dental drill bit (SSW HP-3, SSWhite Burs Inc., Lakewood, NJ). Injections of 2 μl of total volume of each of the viral vectors in sterile PBS at a concentration of 1×10^{12} vg/ml were dispensed into hippocampus and cortex over a period of 4 min using a 26 gauge needle attached to a 10 μl syringe (Hamilton Co., Reno, NV). The incision was then cleaned and closed with surgical staples. Animals were recovered within 10 minutes and housed singly until time of sacrifice.

Immunohistochemistry

Six weeks post surgery, mice were weighed, overdosed with pentobarbital (200 mg/kg;) and perfused with 25 ml of 0.9% normal saline solution then 50 ml of freshly prepared 4% paraformaldehyde. Brains were collected from the animals immediately following perfusion and immersion fixed in 4% paraformaldehyde for 24 h. Mouse brains were cryoprotected in successive incubations in 10%, 20%, 30% solutions of sucrose; 24 h in each solution. Subsequently, brains were frozen on a cold stage and sectioned in the horizontal plane (25 μm thickness) on a sliding microtome and stored in Dulbecco's phosphate buffered saline (DPBS) with 0.2% sodium azide solution at 4 °C.

Six sections 100 μm apart spanning the site of injection were chosen and free-floating immunochemical and histological analysis was performed to determine transgene expression using anti-HA biotinylated rabbit polyclonal antibody at a concentration of 1:1000 (Roche, Indianapolis, IN), total Aβ using a rabbit primary anti-Aß serum at a concentration 1:10,000 and a secondary anti-rabbit antibody (Serotec, Raleigh, NC). Another series of sections were mounted on slides and stained with Congo Red to assess compact congophilic positive plaque load. Immunohistochemical procedural methods are analogous to those described by Gordon et al. 2002, for each marker. Six to eight sections from each animal were placed in multisample staining tray and endogenous peroxidase was blocked (10% methanol, 3% H_20_2, in PBS). Tissue samples were permeabilized (with 0.2% lysine, 1% Triton X-100 in PBS solution), and incubated overnight in appropriate primary antibody. Sections were washed in PBS then incubated in corresponding biotinylated secondary antibody (Vector Laboratories, Burlingame, CA). The tissue was again washed after a 2 h incubation period and then incubated with Vectastin® Elite® ABC kit (Vector Laboratories, Burlingame, CA) for enzyme conjugation. Finally, sections were stained using 0.05% diaminobenzidine and 0.3% H_20_2. For anti-HA 0.5% nickelous ammonium sulfate was added for color enhancement. Tissue sections were then mounted onto slides, dehydrated, and cover slipped. Each immunochemical assay omitted some sections from primary antibody incubation period to evaluate nonspecific reaction of the secondary antibody.

Congo red histology was performed using sections that were premounted on slides then air dried for a minimum of 24 hours. The sections were rehydrated for 30 seconds before beginning staining protocol. For Congo red, hydrated sections were incubated in an freshly prepared alkaline alcoholic saturated sodium chloride solution (2.5mM NaOH in 80% alcohol) for 20 min, then incubated in 0.2% congo red in alkaline alcoholic saturated sodium chloride solution for 30 minutes. Slides with sections were rinsed through three changes of 100% ethanol, and cleared through three changes of xylene and finally coverslipped with DPX. Histological sections from control animals treated with rAAV expressing GFP were mounted on slides and dehydrated through a series of increasing concentrations of ethanol. The mounted sections were then cleared in three changes of histoclear and coverslipped with DPX.

Stained sections were imaged using an Evolution MP digital camera mounted on an Olympus BX51 microscope at 100X final magnification (10 X objective). Six horizontal brain sections (100μm apart; every 4th section) were taken from each animal and four nonoverlapping images near the site of injection from each of these sections were captured (24 measurements per mouse). All images were taken from the same location in all animals. Quantification of positive staining product surrounding and including the injection sites in the right anterior cortex and the right hippocampus and the corresponding regions in the left hemisphere were determined using Image-Pro® Plus (Media Cybernetics®, Silver Springs, MD). Quantifications of the right regions, ispilateral to the injection site, were calculated and ANOVA statistical analysis was performed using StatView® version 5.0.1 (SAS Institute, Raleigh, NC).

Enzyme Activity Assay

ECE activity was characterized and adapted from a previous fluorometric assay method (Johnson and Ahn, 2000) for a 96 well plate format with slight modifications. Six weeks post injection brain tissue was removed then dissected immediately following sacrifice and frozen at −80 °C. The tissue from each animal was rapidly thawed and homogenized with the Ultra-Turrax T8 motor- driven homogenizer (IKA-Labortechnik, Germany) in solubilizing buffer containing 20 mM Tris-HCl, pH 7.4, 250 mM sucrose immediately prior to assaying [40]. Samples were then centrifuged at 100,000 × g, 4 °C for 45 min using an Avanti J-30I Centrifuge (Beckman Instruments, Inc., Palo Alto, CA) to obtain a soluble fraction and a membrane fraction. The membrane fraction was resuspended in buffer containing 20 mM Tris-HCl, 250 mM sucrose, pH 7.4. Protein concentration was determined from the homogenate, membrane fraction and soluble fractions from each sample using a general BCA assay (Pierce). Aliquots of the cell lysate (5 μg) were incubated with 10 μM (final) of the fluorogenic peptide (MOCA-Arg-Pro-Pro-Gly-Phe-Ser-Ala-Phe-Lys(Dnp)-OH), (R&D Systems) in MES buffer (sodium phosphate pH 6.8 containing 0.1M NaCl). MOCA- Arg-Pro-Pro-Gly-Phe-Ser-Ala-Phe-Lys (Dnp)-OH is efficiently quenched by resonance energy transfer to the dinitrophenyl group and the continuous fluorescent intensity is increased upon internal cleavage of the peptide (ECE-1 cleavage between the Ala-Phe bond). The increased fluorescence produced from cleavage of the substrate was measured using a Molecular Devices fMax spectrofluorometer plate reader (MDS Analytical Technologies, Sunnyvale, CA) with a 60 min time point to normalize independent experiments. A standard curve of (7-methoxycoumarin-4-yl) acetyl (MOCA) was analyzed along with each assay and used to convert the relative fluorescence units (RFU) to the moles of MOCA produced by the respective cell lysates. Parallel assay reactions of all samples (in triplicate) were carried out in the presence of an ECE specific inhibitor (SM19712, Sigma Aldrich) at a concentration of 20 μM [49, 50]. ECE specific activity was considered to be the difference in RFU between samples including SM19712 from the total activity samples (no SM19712). Values were calculated and expressed as nanomoles MCA/min/μg protein.

Acknowledgments

Supported by The Johnnie Byrd Center for Alzheimer's Research, NIH grants AG-25509, AG 15490, AG 18478, AG 04418, AG 25711

Reference List

1. Hardy J, Selkoe DJ. The amyloid hypothesis of Alzheimer's disease: progress and problems on the road to therapeutics. Science 2002;297(5580):353–356. [PubMed: 12130773]%19
2. Janus C, Pearson J, McLaurin J, Mathews PM, Jiang Y, Schmidt SD, et al. A beta peptide immunization reduces behavioural impairment and plaques in a model of Alzheimer's disease. Nature 2000;408 (6815):979–982. [PubMed: 11140685]

3. Morgan D, Diamond DM, Gottschall PE, Ugen KE, Dickey C, Hardy J, et al. A beta peptide vaccination prevents memory loss in an animal model of Alzheimer's disease. Nature 2000;408(6815):982–985. [PubMed: 11140686]
4. Westerman MA, Cooper-Blacketer D, Mariash A, Kotilinek L, Kawarabayashi T, Younkin LH, et al. The relationship between Abeta and memory in the Tg2576 mouse model of Alzheimer's disease. J Neurosci 2002;22(5):1858–1867. [PubMed: 11880515]
5. Wilcock DM, Alamed J, Gottschall PE, Grimm J, Rosenthal A, Pons J, et al. Deglycosylated anti-amyloid-beta antibodies eliminate cognitive deficits and reduce parenchymal amyloid with minimal vascular consequences in aged amyloid precursor protein transgenic mice. JNeurosci 2006;26(20): 5340–5346. [PubMed: 16707786]
6. Yan P, Hu X, Song H, Yin K, Bateman RJ, Cirrito JR, et al. Matrix metalloproteinase-9 degrades amyloid-beta fibrils in vitro and compact plaques in situ. JBiolChem 2006;281(34):24566–24574.
7. Mueller-Steiner S, Zhou Y, Arai H, Roberson ED, Sun B, Chen J, et al. Antiamyloidogenic and neuroprotective functions of cathepsin B: implications for Alzheimer's disease. Neuron 2006;51(6): 703–714. [PubMed: 16982417]
8. Turner AJ, Fisk L, Nalivaeva NN. Targeting amyloid-degrading enzymes as therapeutic strategies in neurodegeneration. AnnNYAcadSci 2004;10351−20:1–20.
9. Caccamo A, Oddo S, Sugarman MC, Akbari Y, LaFerla FM. Age- and region-dependent alterations in Abeta-degrading enzymes: implications for Abeta-induced disorders. NeurobiolAging 2005;26(5): 645–654.
10. Yasojima K, Akiyama H, McGeer EG, McGeer PL. Reduced neprilysin in high plaque areas of Alzheimer brain: a possible relationship to deficient degradation of beta-amyloid peptide. NeurosciLett 2001;297(2):97–100.
11. Eckman EA, Eckman CB. Abeta-degrading enzymes: modulators of Alzheimer's disease pathogenesis and targets for therapeutic intervention. BiochemSocTrans 2005;33(Pt 5):1101–1105.
12. Shimada K, Takahashi M, Turner AJ, Tanzawa K. Rat endothelin-converting enzyme-1 forms a dimer through Cys412 with a similar catalytic mechanism and a distinct substrate binding mechanism compared with neutral endopeptidase-24.11. BiochemJ 1996;315(Pt 3):863–867. [PubMed: 8645169]
13. Eckman EA, Watson M, Marlow L, Sambamurti K, Eckman CB. Alzheimer's disease beta-amyloid peptide is increased in mice deficient in endothelin-converting enzyme. JBiolChem 2003;278(4): 2081–2084.
14. Leissring MA, Murphy MP, Mead TR, Akbari Y, Sugarman MC, Jannatipour M, et al. A physiologic signaling role for the gamma -secretase-derived intracellular fragment of APP. ProcNatlAcadSciUSA 2002;99(7):4697–4702.
15. Muller L, Barret A, Etienne E, Meidan R, Valdenaire O, Corvol P, et al. Heterodimerization of endothelin-converting enzyme-1 isoforms regulates the subcellular distribution of this metalloprotease. JBiolChem 2003;278(1):545–555.
16. Hunter AR, Turner AJ. Expression and localization of endothelin-converting enzyme-1 isoforms in human endothelial cells. ExpBiolMed(Maywood) 2006;231(6):718–722.
17. Jackson CD, Barnes K, Homer-Vanniasinkam S, Turner AJ. Expression and localization of human endothelin-converting enzyme-1 isoforms in symptomatic atherosclerotic disease and saphenous vein. ExpBiolMed(Maywood) 2006;231(6):794–801.
18. Eckman EA, Adams SK, Troendle FJ, Stodola BA, Kahn MA, Fauq AH, et al. Regulation of steady-state beta-amyloid levels in the brain by neprilysin and endothelin-converting enzyme but not angiotensin-converting enzyme. JBiolChem 2006;281(41):30471–30478.
19. Burger C, Nash K, Mandel RJ. Recombinant adeno-associated viral vectors in the nervous system. HumGene Ther 2005;16(7):781–791.
20. Mandel RJ, Manfredsson FP, Foust KD, Rising A, Reimsnider S, Nash K, et al. Recombinant adeno-associated viral vectors as therapeutic agents to treat neurological disorders. Mol Ther 2006;13(3): 463–483. [PubMed: 16412695]
21. Gordon MN, Holcomb LA, Jantzen PT, DiCarlo G, Wilcock D, Boyett KW, et al. Time course of the development of Alzheimer-like pathology in the doubly transgenic PS1+APP mouse. Exp Neurol 2002;173(2):183–195. [PubMed: 11822882]

22. Hefti F, Weiner WJ. Nerve growth factor and Alzheimer's disease. AnnNeurol 1986;20(3):275–281.
23. Williams LR, Varon S, Peterson GM, Wictorin K, Fischer W, Bjorklund A, et al. Continuous infusion of nerve growth factor prevents basal forebrain neuronal death after fimbria fornix transection. ProcNatlAcadSciUSA 1986;83(23):9231–9235.
24. Tuszynski MH. Nerve growth factor gene therapy in Alzheimer disease. Alzheimer DisAssocDisord 2007;21(2):179–189.
25. Cenciarelli C, Budoni M, Mercanti D, Fernandez E, Pallini R, Aloe L, et al. In vitro analysis of mouse neural stem cells genetically modified to stably express human NGF by a novel multigenic viral expression system. NeurolRes 2006;28(5):505–512.
26. Fukuchi K, Tahara K, Kim HD, Maxwell JA, Lewis TL, Accavitti-Loper MA, et al. Anti-Abeta single-chain antibody delivery via adeno-associated virus for treatment of Alzheimer's disease. NeurobiolDis 2006;23(3):502–511.
27. Levites Y, Jansen K, Smithson LA, Dakin R, Holloway VM, Das P, et al. Intracranial adeno-associated virus-mediated delivery of anti-pan amyloid beta, amyloid beta40, and amyloid beta42 single-chain variable fragments attenuates plaque pathology in amyloid precursor protein mice. JNeurosci 2006;26 (46):11923–11928. [PubMed: 17108166]
28. Mouri A, Noda Y, Hara H, Mizoguchi H, Tabira T, Nabeshima T. Oral vaccination with a viral vector containing Abeta cDNA attenuates age-related Abeta accumulation and memory deficits without causing inflammation in a mouse Alzheimer model. FASEB J 2007;21(9):2135–2148. [PubMed: 17341681]
29. Hara H, Monsonego A, Yuasa K, Adachi K, Xiao X, Takeda S, et al. Development of a safe oral Abeta vaccine using recombinant adeno-associated virus vector for Alzheimer's disease. JAlzheimersDis 2004;6(5):483–488.
30. Zhang J, Wu X, Qin C, Qi J, Ma S, Zhang H, et al. A novel recombinant adeno-associated virus vaccine reduces behavioral impairment and beta-amyloid plaques in a mouse model of Alzheimer's disease. Neurobiol Dis 2003;14(3):365–379. [PubMed: 14678754]
31. Dodart JC, Marr RA, Koistinaho M, Gregersen BM, Malkani S, Verma IM, et al. Gene delivery of human apolipoprotein E alters brain Abeta burden in a mouse model of Alzheimer's disease. Proc Natl Acad Sci U S A 2005;102(4):1211–1216. [PubMed: 15657137]
32. Marr RA, Rockenstein E, Mukherjee A, Kindy MS, Hersh LB, Gage FH, et al. Neprilysin gene transfer reduces human amyloid pathology in transgenic mice. JNeurosci 2003;23(6):1992–1996. [PubMed: 12657655]
33. Iwata N, Mizukami H, Shirotani K, Takaki Y, Muramatsu S, Lu B, et al. Presynaptic localization of neprilysin contributes to efficient clearance of amyloid-beta peptide in mouse brain. JNeurosci 2004;24(4):991–998. [PubMed: 14749444]
34. Hong CS, Goins WF, Goss JR, Burton EA, Glorioso JC. Herpes simplex virus RNAi and neprilysin gene transfer vectors reduce accumulation of Alzheimer's disease-related amyloid-beta peptide in vivo. Gene Ther 2006;13(14):1068–1079. [PubMed: 16541122]
35. Hemming ML, Patterson M, Reske-Nielsen C, Lin L, Isacson O, Selkoe DJ. Reducing amyloid plaque burden via ex vivo gene delivery of an Abeta-degrading protease: a novel therapeutic approach to Alzheimer disease. PLoSMed 2007;4(8):e262.
36. Mandel RJ, Burger C. Clinical trials in neurological disorders using AAV vectors: promises and challenges. CurrOpinMolTher 2004;6(5):482–490.
37. Alisky JM, Hughes SM, Sauter SL, Jolly D, Dubensky TW Jr. Staber PD, et al. Transduction of murine cerebellar neurons with recombinant FIV and AAV5 vectors. Neuroreport 2000;11(12): 2669–2673. [PubMed: 10976941]
38. Burger C, Gorbatyuk OS, Velardo MJ, Peden CS, Williams P, Zolotukhin S, et al. Recombinant AAV viral vectors pseudotyped with viral capsids from serotypes 1, 2, and 5 display differential efficiency and cell tropism after delivery to different regions of the central nervous system. MolTher 2004;10 (2):302–317.
39. Choi VW, McCarty DM, Samulski RJ. AAV hybrid serotypes: improved vectors for gene delivery. CurrGene Ther 2005;5(3):299–310.
40. Iwata N, Takaki Y, Fukami S, Tsubuki S, Saido TC. Region-specific reduction of A beta-degrading endopeptidase, neprilysin, in mouse hippocampus upon aging. JNeurosciRes 2002;70(3):493–500.

41. Yono M, Latifpour J, Takahashi W, Pouresmail M, Afiatpour P, Weiss RM. Age-related changes in the properties of the endothelin receptor system at protein and mRNA levels in the rat vas deferens. J Recept Signal Transduct Res 2004;24(1−2):53–66. [PubMed: 15344879]

42. Johnson GD, Stevenson T, Ahn K. Hydrolysis of peptide hormones by endothelin-converting enzyme-1. A comparison with neprilysin. J Biol Chem 1999;274(7):4053–4058. [PubMed: 9933597]

43. Lo WD, Qu G, Sferra TJ, Clark R, Chen R, Johnson PR. Adeno-associated virus-mediated gene transfer to the brain: duration and modulation of expression. Hum Gene Ther 1999;10(2):201–213. [PubMed: 10022545]

44. Eckman EA, Reed DK, Eckman CB. Degradation of the Alzheimer's amyloid beta peptide by endothelin-converting enzyme. JBiolChem 2001;276(27):24540–24548.

45. Klein RL, Dayton RD, Tatom JB, Henderson KM, Henning PP. AAV8, 9, Rh10, Rh43 vector gene transfer in the rat brain: effects of serotype, promoter and purification method. MolTher 2008;16(1): 89–96.

46. Burger C, Nguyen FN, Deng J, Mandel RJ. Systemic mannitol-induced hyperosmolality amplifies rAAV2-mediated striatal transduction to a greater extent than local co-infusion. Mol Ther 2005;11 (2):327–331. [PubMed: 15668145]

47. Zolotukhin S, Potter M, Zolotukhin I, Sakai Y, Loiler S, Fraites TJ Jr. et al. Production and purification of serotype 1, 2, and 5 recombinant adeno-associated viral vectors. Methods 2002;28(2):158–167. [PubMed: 12413414]

48. Holcomb L, Gordon MN, McGowan E, Yu X, Benkovic S, Jantzen P, et al. Accelerated Alzheimer-type phenotype in transgenic mice carrying both mutant amyloid precursor protein and presenilin 1 transgenes. NatMed 1998;4(1):97–100.

49. Umekawa K, Hasegawa H, Tsutsumi Y, Sato K, Matsumura Y, Ohashi N. Pharmacological characterization of a novel sulfonylureid-pyrazole derivative, SM-19712, a potent nonpeptidic inhibitor of endothelin converting enzyme. Jpn J Pharmacol 2000;84(1):7–15. [PubMed: 11043447]

50. Matsumura Y, Kuro T, Kobayashi Y, Umekawa K, Ohashi N, Takaoka M. Protective effect of SM-19712, a novel and potent endothelin converting enzyme inhibitor, on ischemic acute renal failure in rats. Jpn J Pharmacol 2000;84(1):16–24. [PubMed: 11043448]

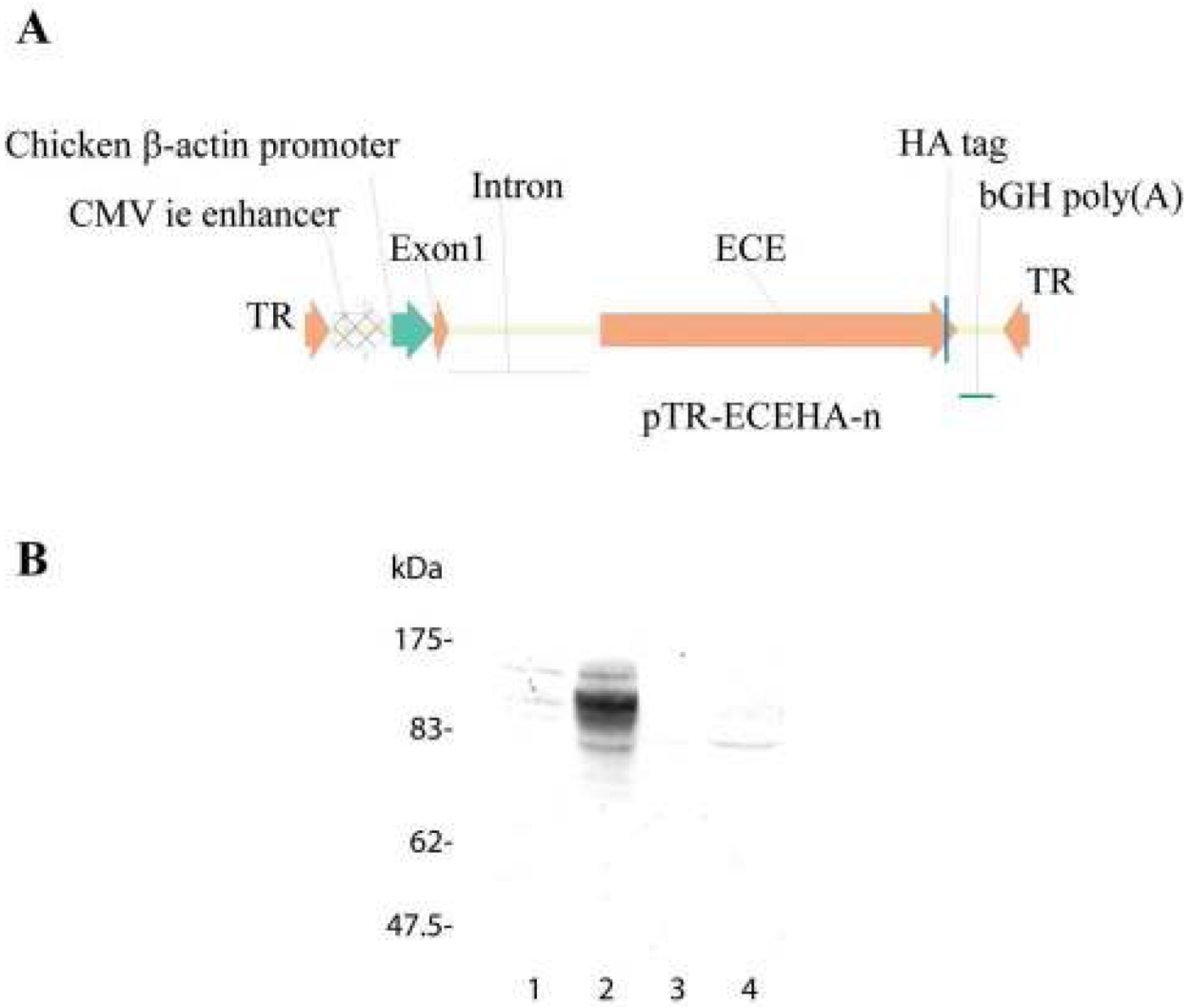

Figure 1. Diagram of ECE construct and Western analysis of ECE expression in HEK 293 cells

(A) Diagrammatic representation of rAAV construct expressing the ECE cDNA under the control of the chicken β-actin (CBA) promoter. (B) Western analysis of ECE expressed in 293 cells using an anti-HA antibody. Lane 1, 293 cell lysate; lane 2, ECE transfected cell lysate, lane 3, conditioned media from untransfected cells, lane 4 media from cells transfected with ECE.

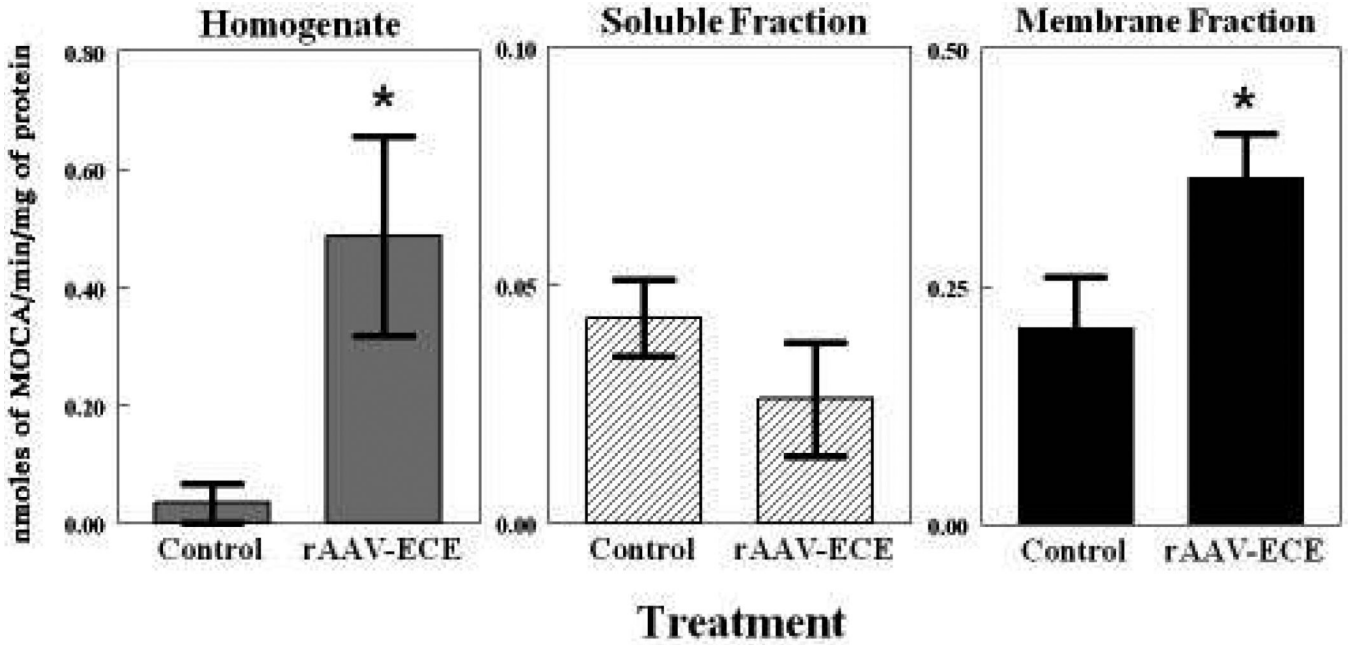

Figure 2. ECE enzymatic activity obtained from mice hippocampal regions after injection of rAAV virus expressing ECE protein

ECE-like specific activity is higher in the membrane fraction and homogenate of the hippocampal tissue in the ECE treatment group compared to the control group. The star (*) indicates significance with a p-value < 0.05. Error bars indicate standard error of the mean value (specific activity/min/μg protein) for each treatment group (n=6 per group).

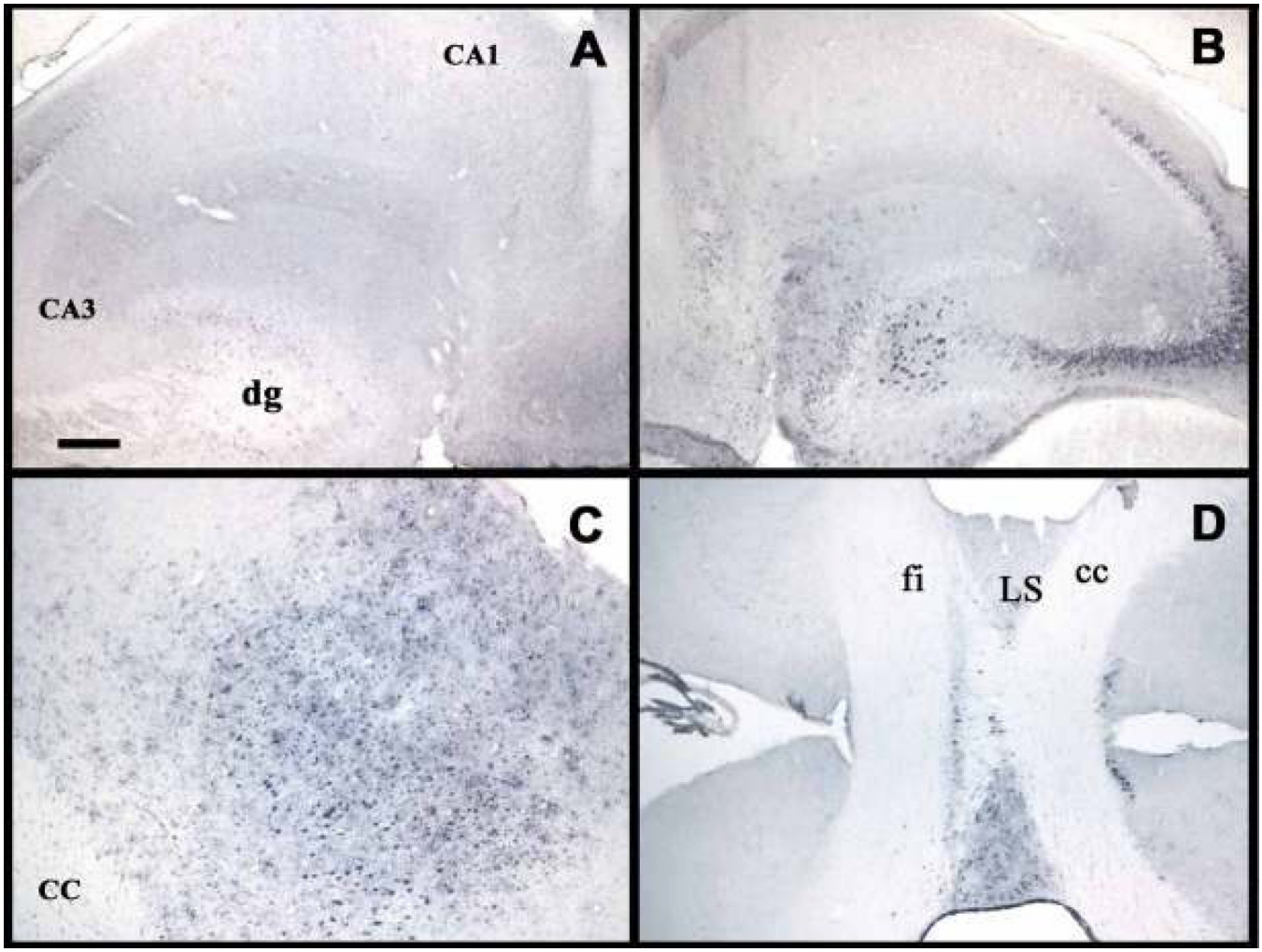

Figure 3. Examination of ECE expression using anti-HA immunoreactivity in the hippocampus and anterior cortex

Panel A shows slight ECE expression in granule cells of the dentate gyrus of the left contra lateral hippocampus following intracranial administration of ECE into the right hippocampus. Panel B shows strong ECE expression detected at the site of vector injection. Panel C shows strong ECE expression in the anterior cortex. Panel D shows slight ECE expression along the midline and some expression in the lateral septum of left (contra lateral) side following intracranial administration of ECE into the right anterior cortex. fi = fimbtria; LS = lateral septum; CC = corpus callosum; dg = dentate gyrus; CA1 = Cajal Area 1; CA3 = Cajal area 3; Magnification = 40X and Scale bar = 120μm.

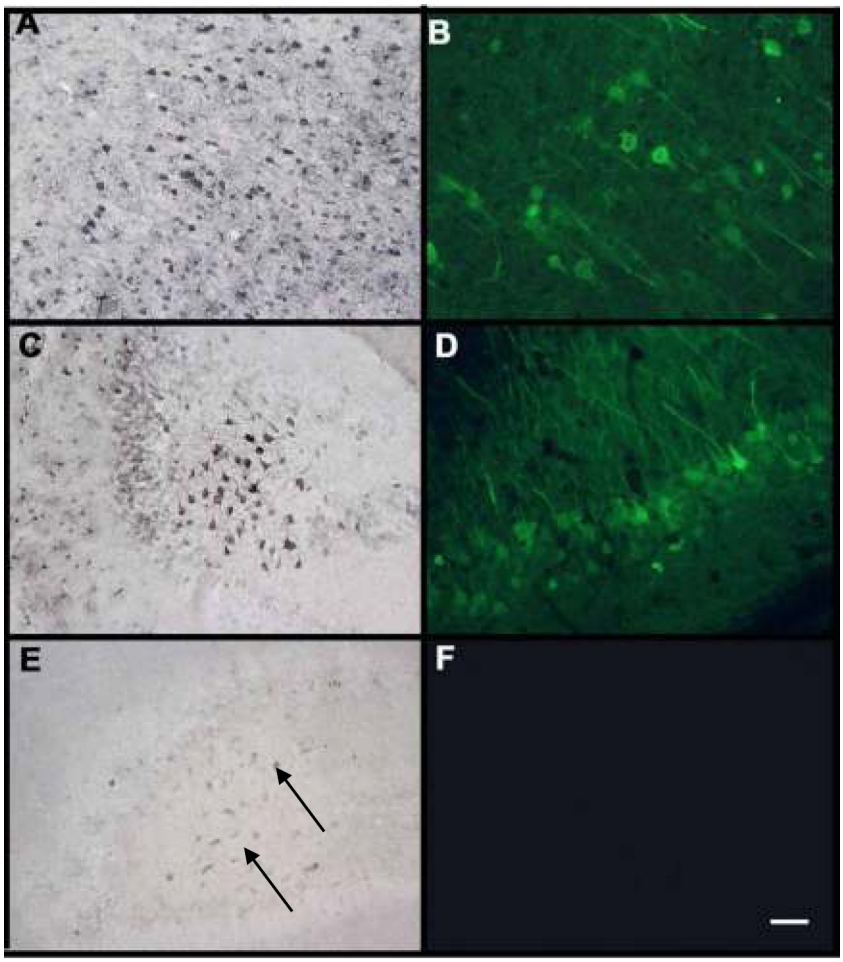

Figure 4. ECE and GFP expression profiles in mice brains

Panels A shows strong ECE expression in the right anterior cortex following intracranial administration of ECE vector. Panel B shows GFP expression in the anterior cortex following intracranial administration of control GFP vector. Panel C shows ECE expression in pyramidal cells in CA2 region of the right hippocampus. Panel D shows GFP expression in the CA3 region of the hippocampus. Panel E shows slight ECE expression in CA4 neurons of the dentate gyrus of the left contra lateral hippocampus. Panel F shows no positive expression in the left uninjected hippocampus following intracranial injection of GFP vector into the right hippocampus. Scale bar = 50μm (panels A, C, E). Scale bar = 25 μm (panels B, D, F).

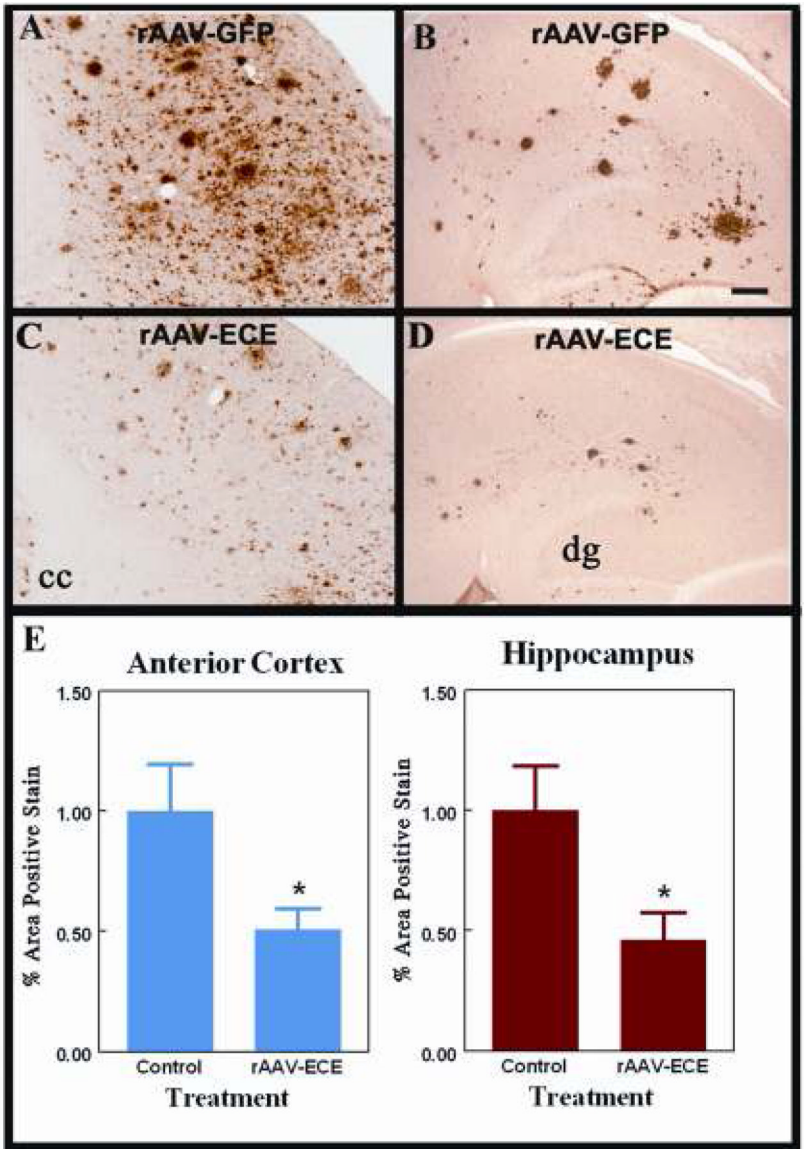

Figure 5. Total amyloid load is reduced following intracranial administration of AAV-ECE vector

Panels A and B show Aβ immunostaining in the right cortex and hippocampus respectively of animals receiving intracranial injection of control vector, GFP. Panels C and D show Aβ immunostaining in right cortex and hippocampal regions respectively of mice receiving intracranial injection of ECE. Scale bar = 120μm. Panel G shows the percent area of positive staining, normalized to the control, for both cortex (left) and hippocampus (right) after AAVECE injection. The asterisk (*) indicates significant reduction compared with control values with p-values < 0.05.

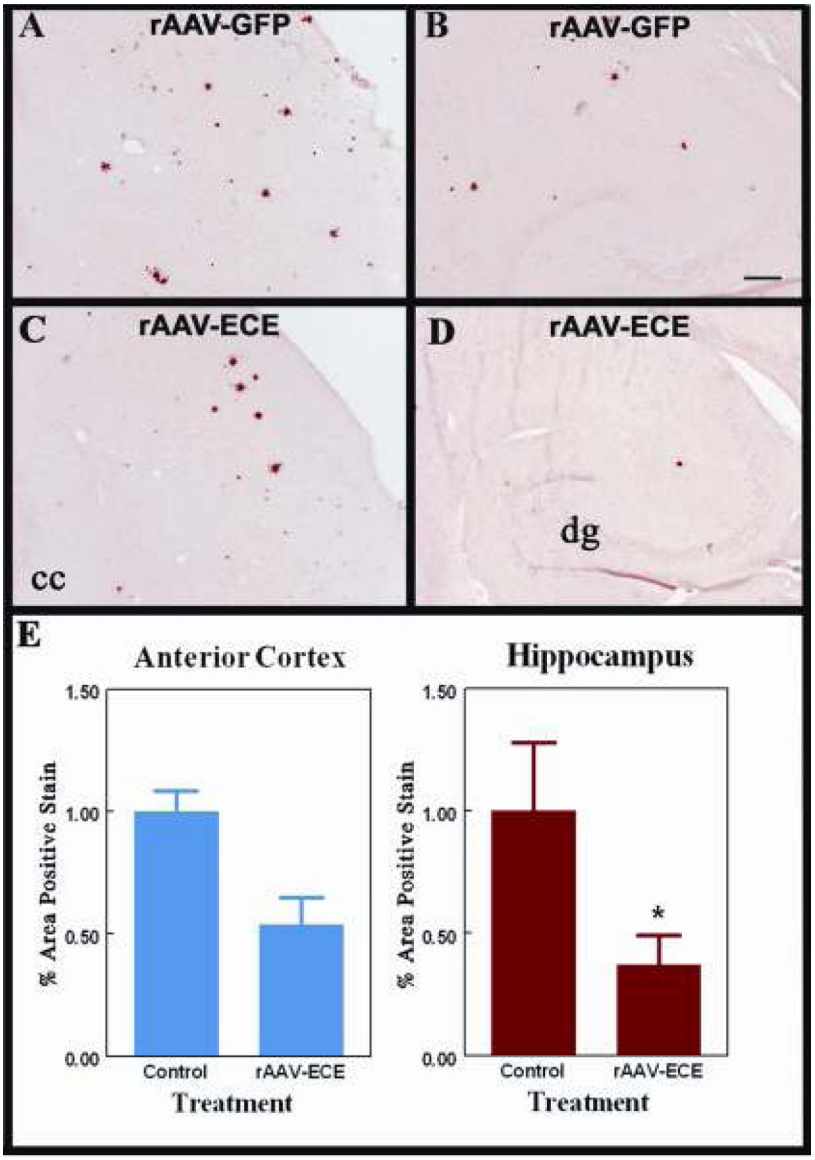

Figure 6. Congophilic compact plaque load is reduced following intracranial administration of ECE AAV vector

Panels A and B show total congophilic staining in the right cortex and hippocampus respectively of animals receiving intracranial injection of control vector, GFP. Panels C and D show congophilic positive staining in right cortex and hippocampal regions respectively of mice receiving intracranial injection of ECE. Magnification = 40X, scale bar = 120μm. Panel E shows the percent area of positive staining, normalized to the control, for the cortical (right) and hippocampal (left) injected regions. The star (*) indicates significance with a p-value < 0.05.